



Characterization of water hyacinth cellulose-g-poly(ammonium acrylate-co-acrylic acid)/nano-hydroxyapatite polymer hydrogel composite for potential agricultural application

Kiplangat Rop^{a,*}, Damaris Mbui^a, George N. Karuku^b, Immaculate Michira^a, Njagi Njomo^a

^a Department of Chemistry, University of Nairobi. P.O. Box 30197-00100, Nairobi, Kenya

^b Department of Land Resource Management and Agricultural Technology, University of Nairobi, P. O. Box 29053-00625, Kangemi, Nairobi, Kenya

ARTICLE INFO

Article history:

Received 2 September 2019

Accepted 2 December 2019

Available online xxx

Keywords:

Polymer

Nano-composite

Nano-hydroxyapatite

Swollen cellulose

Water hyacinth

Moisture retention

ABSTRACT

Polymer nano-composite was prepared by grafting partially neutralized acrylic acid onto swollen cellulose isolated from water hyacinth in the presence of nano-hydroxyapatite (nano-HA) using *N,N*-methylene-bis-acrylamide (MBA) as the cross-linker and ammonium persulphate (APS) as the free radical initiator. Water absorption tests showed an increase in swelling ratio of the copolymer with increased nano-HA content to value of 120 g/g at 2.5% w/v above which it declined. FTIR spectrum of nano-composite revealed grafting of the monomer (acrylic acid/ammonium acrylate) onto cellulose and nano-HA. Transmission electron microscopy (TEM) images of nano-HA synthesized in the presence of Triton X-100 (non-ionic surfactant) displayed rod-shaped agglomerates and nano-particle dispersion within the copolymer matrix. Energy dispersive X-ray (EDX) spectra revealed the constituents of nano-composite to be mainly C, O, Ca and P, while N was not detected by this method. X-ray diffractograms (XRD) of cellulose grafted copolymer showed a more amorphous structure relative to that of dry water hyacinth cellulose and also presence of crystalline nano-HA within the copolymer. This polymer nano-composite could be beneficial in agriculture in aiding moisture retention as well as a source of P which occurs through microbial degradation of cellulose grafted copolymer and solubilization of nano-HA.

© 2019 The Author(s). Published by Elsevier B.V. This is an open access article under the CC BY-NC-ND license (<http://creativecommons.org/licenses/by-nc-nd/4.0/>).

1. Introduction

Polymer hydrogels (PHGs) are 3 dimensional network materials which can absorb and retain large amounts of water due to presence of hydrophilic groups such as $-\text{COOH}$, $-\text{CONH}_2$, $-\text{SO}_3\text{H}$ and cross-links formed by covalent, electrostatic, hydrophobic bonds, that resist dissolution [1–3]. These characteristics enable extensive applications in food industry as thickening agents, bio-medicine as artificial organs, agriculture as soil conditioners, pharmaceuticals in controlled drug delivery and hygiene as sanitary towels and baby diapers, among others [2,4]. Majority of these polymers are prepared from petro-chemicals and due to high cost of monomers, there has been growing pressure to produce them using renewable natural resources such as starch, cellulose, chitosan, alginate, pectin, carrageenan, collagen and lignin [4,5]. Other challenges associated with the use of PHGs are low mechanical strength and poor degradability [4,6]. For instance, linear and cross-linked polyacrylamide (PHGs) is used as a soil conditioner to improve

moisture retention and stabilize soil aggregates in order to minimize crust formation and soil erosion; though its degradation rate in soil is $<10\%$ per year [7]. These challenges can be alleviated by cross-linking vinyl monomers with biodegradable materials such as cellulose. Cellulose attracts much attention due to its abundance, low cost and exceptional properties such as biodegradability, biocompatibility, hydrophilicity, nontoxicity, among others. Cellulose-based PHGs are often prepared using cellulose derivatives such as carboxymethyl cellulose by free radical polymerization technique [8,9]. The monomers commonly employed include acrylic acid and its salts, acrylamide and methacrylamide [10,11].

Water absorbency and retention properties of PHGs attract much interest for use in agriculture as slow release fertilizer (SRF) carriers and soil conditioners [3]. About 40–70% N, 80–90% P and 50–70% K of applied conventional fertilizers are lost to the environment through surface runoff, leaching and volatilization causing serious economic losses and environmental pollution [2,12]. These losses can be reduced by encapsulating the nutrients within a biodegradable PHG as delivery vehicle to synchronize nutrient release with plant uptake subsequently reducing negative environmental impact associated with conventional fertilizer application. PHGs can also improve soil moisture retention capacity thus reducing cost of irrigating crops particularly in arid and

* Corresponding author.

E-mail addresses: kiplangatrop@uonbi.ac.ke (K. Rop), dmbui@uonbi.ac.ke (D. Mbui), gmoe54321@gmail.com (G.N. Karuku), imichira@uonbi.ac.ke (I. Michira), njaginjomo@uonbi.ac.ke (N. Njomo).

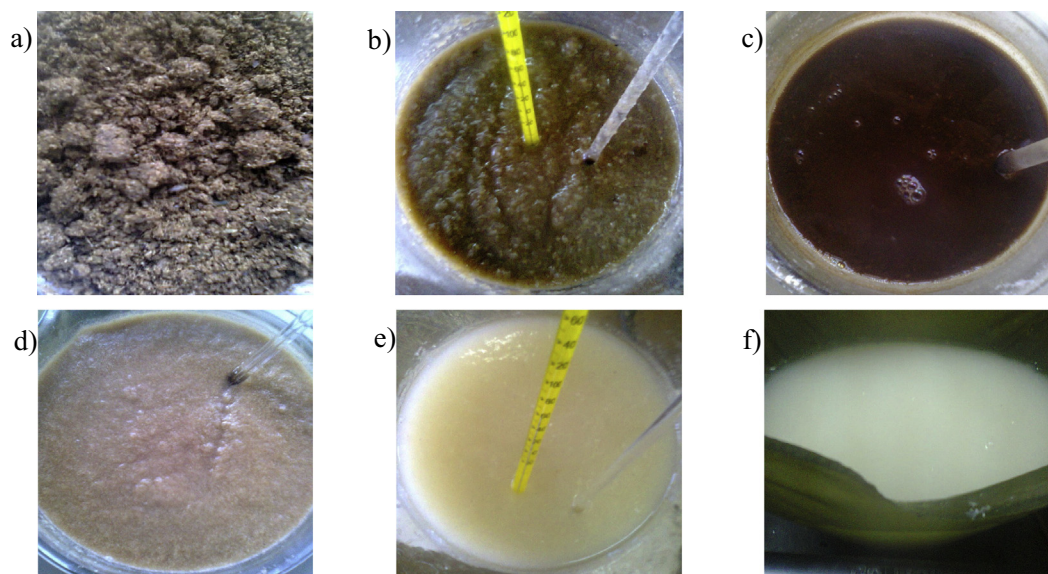


Fig. 1. Summary of the procedure of isolating cellulose from water hyacinth: (a) solvent extracted water hyacinth, (b) 1st bleaching (c) alkaline hydrolysis (d) 2nd bleaching (e) acid hydrolysis (f) washing.

semi-arid lands (ASALs). However, high cost of producing PHGs limits their application in various fields including agriculture and efforts have been made to overcome this challenge by developing polymer nano-composites using inorganic fillers (clay minerals) such as kaolinite [7], montmorillonite [13,14], bentonite [15], attapulgite (Palygorskite) [16] and clinoptilolite [17]. These clay minerals are attractive due to their abundance in nature and other exceptional properties such as high specific surface area, high cation exchange capacity, physical-chemical stability and high intercalation.

The formulation SRFs mainly involves charging the copolymer with soluble fertilizers such as urea, $(\text{NH}_4)_2\text{HPO}_4$ and KH_2PO_4 [14,17]. However, high solubility urea and inorganic salts could limit slow release property when chemical interaction does not exist between the nutrients and the delivery material. Available publications on the SRFs formulation focus mainly on N. Few studies consider elements such as P which is prone to erosion loss and fixation into plant unavailable forms by certain soil types such as the nitisols [18]. Recent studies on SRFs formulation using nano-HA demonstrate the potential to enhance P use efficiency. Lui and Lal [19] observed better mobility of carboxymethyl cellulose (CMC)-stabilized nano-HA in soil compared to nano-HA without CMC, suggesting a more efficient delivery of P to the root system. This nano-fertilizer formulation improved growth and yield of soybeans, above those of CaHPO_4 treatment. Montalvo et al. [20] evaluated efficiency of nano-HA (20 nm) in strong P-sorbing andisols and oxisols, relative to bulk HA (600 nm). They observed greater mobility of nano-HA in andisol than oxisol and P could not be recovered in the leachates in both soil types for bulk HA due to large particle size. The P uptake and the % P in wheat (*Triticum aestivum*) derived from the fertilizers in both soil types followed the order; TSP > nano-HA > bulk HA.

Nano-HA can be incorporated into PHG to form a polymer nano-composite for slow release of phosphate. The active -OH groups on the surface of nano-HA can react with the monomer forming part of the network besides being physically trapped within the copolymer. This current study, attempted to prepare a polymer nano-composite fertilizer by grafting partially neutralized acrylic acid onto cellulose derived from water hyacinth (WH) in the presence of nano-HA. The formulated product was characterized for potential agricultural application as a SRF and soil conditioner, particularly in arid/semi arid areas where water retention and release is essential. The release of P from polymer nano-composite into the soil is considered to depend on

microbial degradation of the copolymer and solubilization of nano-HA, and subsequent diffusion of P.

2. Materials and methods

2.1. Materials

Acrylic acid and *N,N*-methylene-bis-acrylamide were obtained from ACROS Organics, Germany. All other chemicals such as ammonium persulphate, toluene, ethanol, sodium hydroxide, hydrochloric acid, acetone, calcium hydroxide, orthophosphoric acid and ammonia were obtained from Loba Chemie, Mumbai, India.

2.2. Extraction of cellulose from water hyacinth

Cellulose was isolated from water hyacinth (*Eichhornia crassipes*) as previously described [21]. The extraction procedure is summarized in Fig. 1; where, dry water hyacinth was treated with ethanol/toluene (2:1 v/v) to extract compounds other than cellulose, hemicellulose and lignin (Fig. 1a). Hemicellulose and lignin were removed by bleaching with NaOCl, alkaline (aqueous NaOH) and acid (5% HCl) hydrolysis (Fig. 1b, c, d & e), and then washing to remove the acid (Fig. 1f).

2.3. Synthesis of nano-hydroxyapatite (nano-HA)

Nano-HA was synthesized following the procedure adopted by Rop et al. [22] in which $\text{Ca}(\text{OH})_2$ and H_3PO_4 were reacted both in the presence and in the absence of a surfactant (TX-100) under mechanical agitation (1000 rpm). The stoichiometric ratio of Ca:P was maintained at 1.67 according to Scheme 1. Nano-particles formed were oven-dried at 105 °C to constant weight and then pulverized to fine powder. The surfactant was removed by washing the nano-HA powder with methanol.



Scheme 1. Reaction between orthophosphoric acid and calcium hydroxide to yield nano-HA

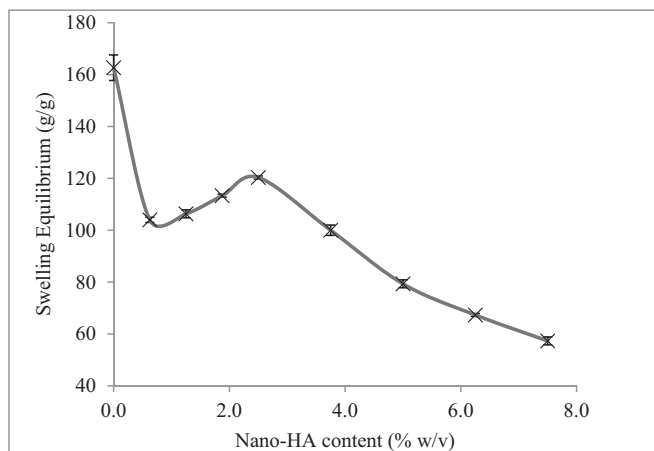


Fig. 2. Effect of nano-HA content on the water absorbency of cellulose grafted PHG, the values are reported as mean \pm SD ($n = 3$).

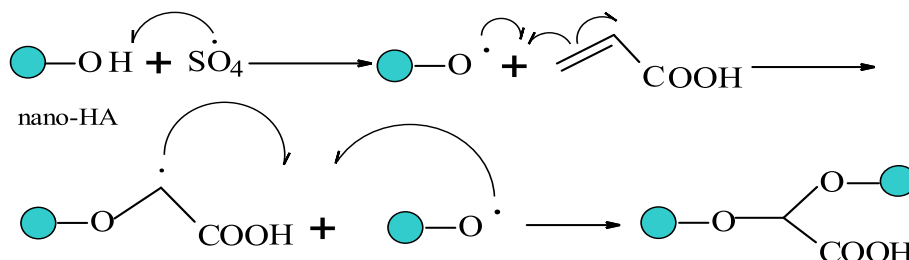
2.4. Preparation of cellulose-g-poly(ammonium acrylate-co-acrylic acid)/ nano-HA composite

30 mL of swollen cellulose (2.67%w/v) and 0.25 g nano-HA powder was transferred into a 3-necked flask fitted with a reflux condenser and nitrogen. The flask was placed in a thermostated water bath equipped with a magnetic stirrer. Nitrogen gas was bubbled through the mixture for 10 min as the temperature was raised to 70 °C. 0.1 g of APS was added into the mixture with stirring for 30 min to generate radicals. 2.7 mL of acrylic acid neutralized with NH_3 to 70% (degree of neutralization) and 0.25 g of *N,N*-methylene-bis-acrylamide were mixed in a beaker, stirred to dissolve and then introduced into the reaction flask. The total volume of the reaction mixture was adjusted to 40 mL using distilled water. Stirring was continued for 1 min and then stopped, and the reaction mixture left to stand for 2 h. The reaction product was allowed to cool to room temperature, removed from the flask and then cut into small pieces. These pieces were soaked in distilled water and a 1:1 NH_3 solution added drop-wise to adjust the pH to 8. It was Soxhlet extracted with acetone for 2 h to remove homopolymer, oven dried at 60 °C to a constant weight, pulverized and tested for water absorption. The same procedure was repeated for 0.5, 0.75, 1.0, 1.25, 1.5, 2.5 and 3.0 g of nano-HA.

2.5. Water absorption tests

A 0.1 g sample of powdered polymer nano-composite was placed in a porous bag, immersed in distilled water and allowed to swell to equilibrium at room temperature. The swollen sample was gently dabbed with filter paper to remove surface water and the weight taken. Swelling ratio was determined using the following equation.

$$\text{SEQ} = \left(\frac{W_{eq} - W^{\circ}}{W^{\circ}} \right)$$



Scheme 2. Grafting of acrylic acid (monomer) onto nano-HA by chain transfer mechanism

where, W° (g) is the weight of dry polymer nano-composite, W_{eq} (g) is the weight of swollen polymer nano-composite at equilibrium and SEQ (g/g) is the swelling ratio (water absorbency) at equilibrium.

2.6. Structural and morphological characterization

2.6.1. FTIR spectroscopy

FTIR spectrophotometer (Shimadzu IRAffinity-1S) was used to characterize isolated water hyacinth (WH) cellulose, cellulose-grafted PHG and polymer nano-composite. The sample holder was cleaned and the background scanned without the sample. A pulverized sample was placed on the sample holder, pressed against the diamond crystal and then scanned between 4000 cm^{-1} and 500 cm^{-1} .

2.6.2. Transmission electron microscopy and energy dispersive X-ray (EDX) spectroscopy

The morphology of copolymers was investigated using high resolution transmission electron microscope (HRTEM), Tecnai G2 F20 X-TWIN MAT instrumentation at an operating voltage of 200 kV, and equipped with energy dispersive X-ray (EDX) spectrometer.

2.6.3. X-ray diffraction (XRD) analysis

1 g of the sample was placed in a disc with an internal diameter of 1.5 cm. X-ray diffractograms were recorded using D2 PHASER (Bruker) with $\text{Cu K}\alpha$ radiation (1.54184 Å) and a generator working at a voltage of 30 kV and a filament current of 10 mA. The samples were scanned from $2\theta = 8^{\circ}$ to 40° at the rate of 0.090°/min.

3. Results and discussion

3.1. Characteristics of isolated cellulose

The isolated cellulose fibres were dispersed in water (Fig. 1f) suggestive of the exposure of hydrophilic -OH groups. The swelling of cellulose was ascribed to loosened hydrogen bonding scheme due to alkaline treatment and bleaching, and also decreased crystallinity of cellulose that expanded the amorphous region [23–25]. This is a vital prerequisite to render the system accessible to reagents in the heterogeneous chemical reaction.

3.2. Effect of nano-HA content on water absorbency of cellulose grafted polymer hydrogel

The effect of nano-HA content on water absorbency (SEQ) of cellulose grafted copolymer is presented in Fig. 2. The polymer without nano-HA synthesized by grafting 6.75% (w/v) partially neutralized acrylic acid onto 2% (w/v) cellulose, could swell in distilled water up to 163 g/g (Fig. 2). The SEQ initially decreased on introducing nano-HA from 163 to 104 (g/g) followed by a marked increase up to an optimal value of 120 (g/g) at 2.5% w/v, after which it declined. The decrease may be attributed to the rigidity of nano-HA which occupied the voids within the copolymer network, decreasing the free volume for accommodating water molecules. The subsequent increase in SEQ could be attributed to -OH groups at the surface nano-HA which enhanced the

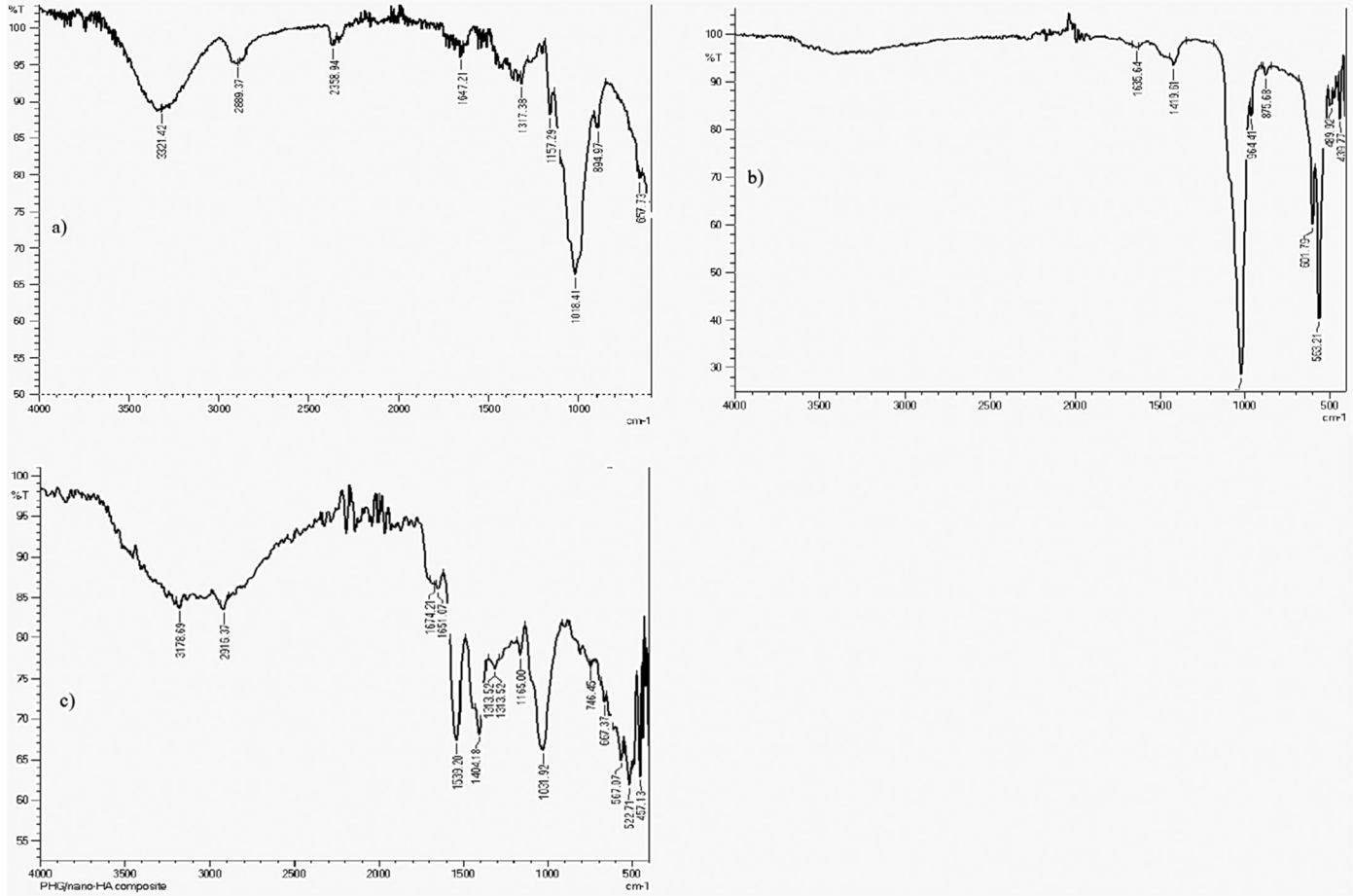
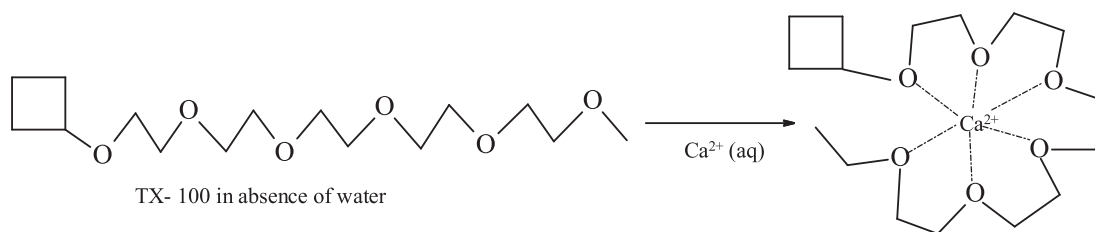


Fig. 3. FTIR spectra of (a) water hyacinth cellulose, (b) nano-HA and (c) cellulose graft poly(acrylamide-co-acrylic acid)/nano-HA composite.



Scheme 4. The ion-dipole interaction between Ca^{2+} and polyoxyethylene group of TX-100 leading to formation of hydrophobic complex [28]

hydrophobic ring complex formed through ion-dipole interaction between Ca^{2+} and polyoxyethylene group of TX-100 according to Scheme 4. The formation of this complex is thought to reduce the transfer rate of Ca^{2+} to the growing crystals thereby reducing nano-particle size under controlled conditions. The formation of nano-rods is also attributed to adsorption of TX-100 onto certain planes of formed crystals leading to growth of nano-particles in a preferential direction. The agglomeration of nano-particles (Fig. 4a & b) was attributed to high specific surface energy that led to aggregation [32,33]. TEM images of nano-composite (Fig. 4c) showed dispersion of nano-HA within the copolymer. Similarly, Ragu and Sakthivel [33] observed diminished agglomeration of nano-HA in polymethyl methacrylate/nano-HA

composite at about 20 to 50 nm, an observation attributed to reduction of surface energy of nano-HA by the polymer through its pendent PO_4^{3-} group.

3.5. Energy dispersive X-ray (EDX) spectroscopy

The energy dispersive X-ray (EDX) spectra of the cellulose grafted copolymer, nano-HA and polymer nano-composite are shown in Fig. 5. The spectrum of cellulose grafted copolymer (Fig. 5a) revealed an intense carbon band at 0.2 KeV due to cellulose and acrylic chains being the main constituents of the copolymer. Other elements detected were oxygen (0.5 KeV) due to cellulose, sulphur (2.3 KeV) due to

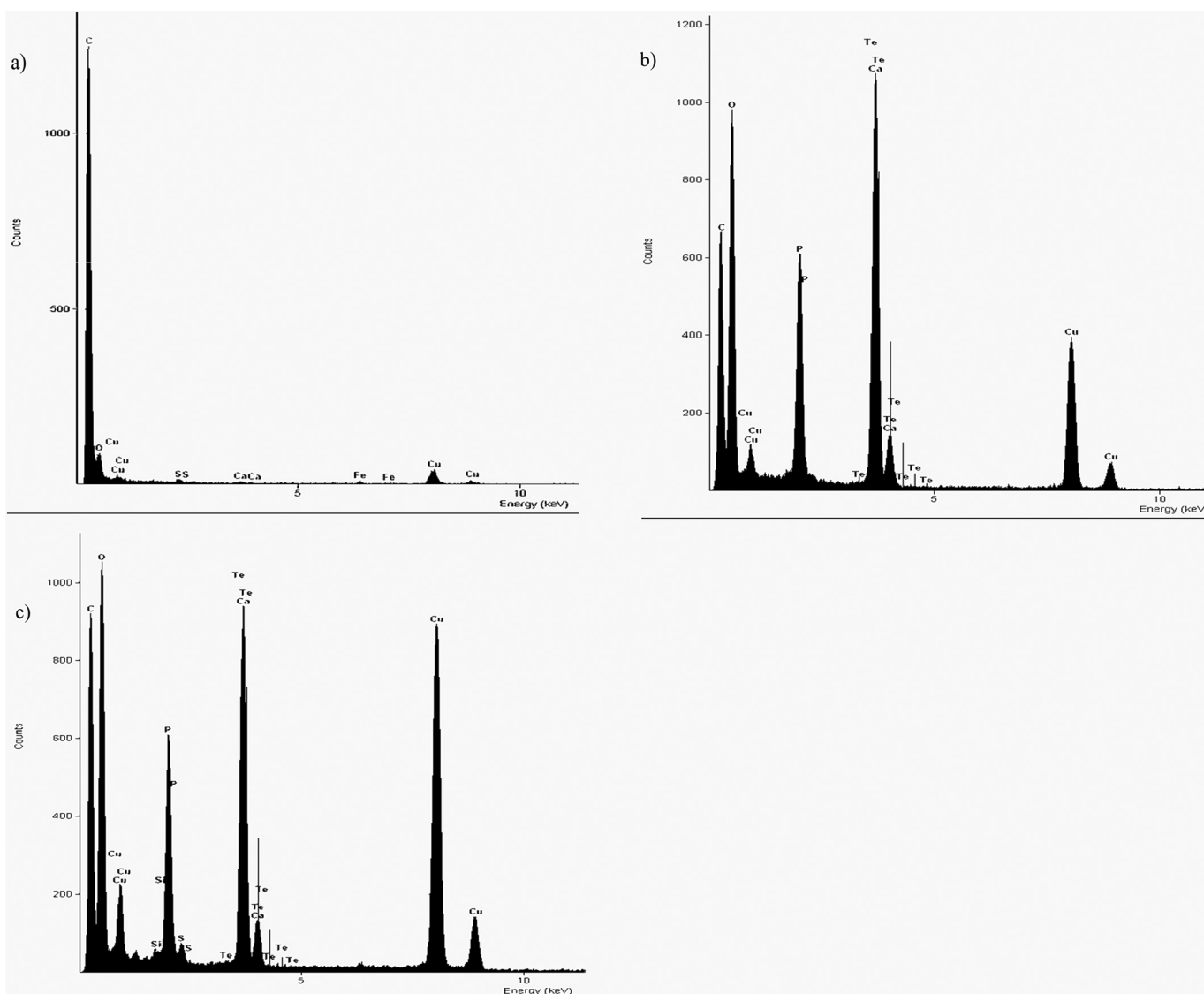


Fig. 5. EDX spectra of (a) cellulose-g-poly(acrylamide-co-acrylic acid), (b) nano-HA, (c) cellulose-g-poly(acrylamide-co-acrylic acid)/nano-HA.

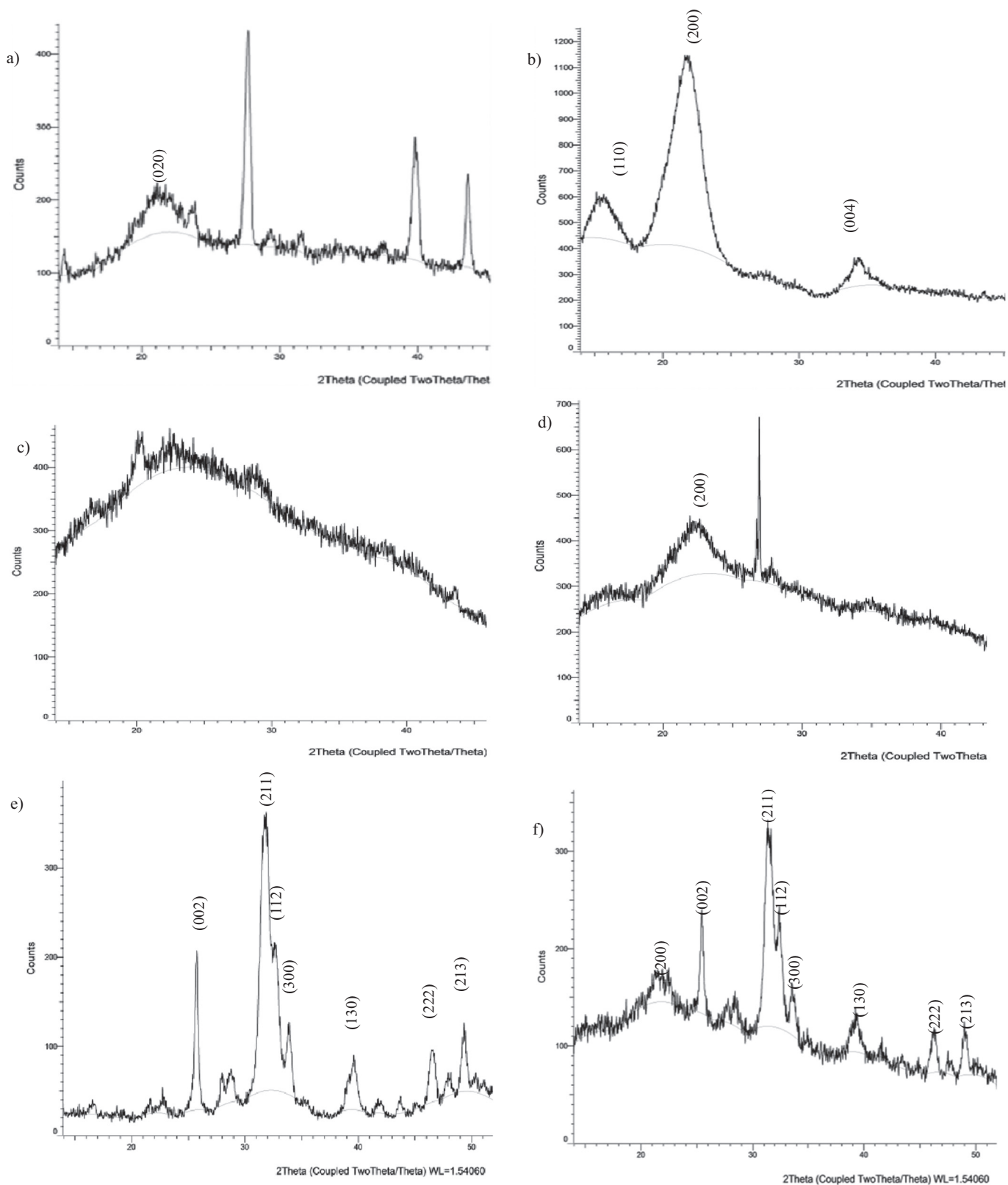
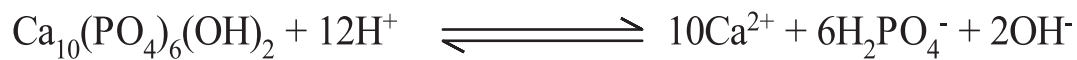


Fig. 6. Diffractograms of (a) crude water hyacinth, (b) isolated dry cellulose, (c) PHG without cellulose, (d) cellulose grafted PHG, (e) nano-HA, (f) cellulose-g-poly(acrylamide-co-AA)/nano-HA composite.



Scheme 5. Neutralization reaction for the dissolution of nano-HA in acidic environment

ammonium persulphate (radical initiator), Cu (0.9, 8 & 9 KeV) due to the grid used during viewing, while Ca (3.7 KeV) and Fe (6.4 & 7 KeV) could be part of the nutrients absorbed by the WH during growth. The band characteristic of N was not observed as expected and this could be due to absorption by the detector window. The X-ray transmission by Beryllium window is almost 100% for energies >2 KeV, but it drops to about zero at 0.5 KeV [34], hence X-ray line such as that of N (0.4 KeV) is absorbed. The presence of carbon in the sample is also implicated for low detection of N K α (X-ray line) because of high mass absorption coefficient value of 25,500 cm² g⁻¹ [34].

Nano-HA spectrum (Fig. 5b) displayed the main constituents of sample as calcium (3.7 KeV), phosphorous (2.0 KeV), oxygen (0.5 KeV) and carbon (0.2 KeV). Ca, P and O are expected in nano-HA lattice, while C may be attributed to the existence of CO₃²⁻ ions. Cisneros-Pineda et al. [30] also obtained a peak due to carbon and attributed it to sensitivity of apatite lattice to the substitution environment of the CO₃²⁻ ions. This substitution can either be type A where CO₃²⁻ ions replace —OH ions, or type B where the CO₃²⁻ ions replace PO₄³⁻ ions [30]. Similar bands were observed in polymer nano-composite (Fig. 5c), but the peaks were more intense than those observed in nano-HA spectrum due to oxygen and carbon (Fig. 5b), an observation attributable to cellulose grafted copolymer fraction. Sulphur was also detected in polymer nano-composite due to ammonium persulphate (radical initiator). The rest of peaks due to Cu (0.9, 8.0 & 9.0 KeV) may have originated from the grid, Te (3.8 KeV) and Si (1.8 KeV) are not related to the constituents of the sample and could have probably originated from metal conductive layers and/or impurities.

3.6. X-ray diffraction (XRD) analysis

The X-ray diffraction patterns of WH, isolated dry cellulose, copolymer without cellulose, cellulose grafted copolymer, nano-HA and polymer nano-composite are presented in Fig. 6. The crude WH (Fig. 6a) displayed diffraction peaks at $2\theta = 21.6^\circ$ corresponding to (020) crystallographic plane reflections characteristic of cellulose I, and bands at $2\theta = 26.5^\circ, 39.5^\circ$ and 44° that could be related to cellulose I β structure. The isolated cellulose (Fig. 6b) indicated diffraction peaks at $2\theta = 16^\circ, 22^\circ$ and 34.5° assigned to (110), (200) and (004) crystallographic plane reflections for cellulose I, respectively. The findings are in agreement with those of [35–40]. The intense peaks observed in isolated (mercerized) dry cellulose (Fig. 6b) may be attributed to restructured H-bonds (coalescence) that increased crystallinity of cellulose [25,38,39]. The copolymer without cellulose (Fig. 6c) displayed an amorphous pattern. Cellulose grafted copolymer (Fig. 6d) showed a diffraction band of lower intensity at $2\theta = 22^\circ$ (200) for cellulose I crystalline allomorph, relative to the intensity of the same peak in the isolated cellulose (Fig. 6b), confirming grafting of monomers onto cellulose. The diffraction band in cellulose grafted copolymer at $2\theta = 26.5^\circ$ (Fig. 6d) is suggestive of the existence of some crystalline cellulose allomorph that was not fully destroyed during alkali treatment, limiting the accessibility of —OH groups during the polymerization reaction. Nano-HA displayed mainly diffraction bands at $2\theta = 26^\circ, 32^\circ, 33^\circ, 34.3^\circ, 39.5^\circ, 46.5^\circ, 49.5^\circ$ (Fig. 6e) assigned to (002), (211), (112), (300), (130), (222), (213) crystallographic plane reflections, respectively [29,31,33,41,42]. The cellulose grafted polymer/nano-HA composite (Fig. 6f) indicated a weak diffraction band at around $2\theta = 22^\circ$ (200) attributed to cellulose I allomorph, with the rest of the bands being typical of nano-HA crystalline structure.

The degradation of the copolymer in soil and by soil microbial isolates, and the potential agricultural implication of nano-composite were carried out in separate studies [21,22,43]. The authors observed enhanced degradation of cellulose grafted copolymer in soil microbial culture relative to copolymer without cellulose [21]. Soil amended with cellulose grafted copolymer showed statistically significant soil mineral N content during 16 weeks incubation period relative to untreated soil, an observation ascribed to hydrolysis of amide-N. The pH

of soil amendments in the 2nd week of incubation ranged from 5.15–5.33 which increased to values ranging from 5.71–5.97 as at 16th week [22]. This was largely attributed to the release of Ca²⁺ ions which have the effect of neutralizing the acids. Polymer nano-composite released solubilized P from nano-HA which is thought to mainly depend on microbial action [22]. Soil bacterial species such as *Pseudomonas*, *Anthrobactor* and fungi such as *Aspergillus*, *Penicillium*, are implicated for solubilization of insoluble phosphates such as apatite [44,45]. They secrete low molecular weight organic acids such as citric, gluconic, lactic, oxalic and acetic acids to lower the pH and chelate mineral ions. The acidification of soil microbial environment as well as rhizosphere environment by plant root exudates under P limitation, is considered to solubilize nano-HA according to Scheme 5 [43]. According to the law of mass action, equilibrium shift to the right (solubilization) is favored by increased concentration of H⁺ and continuous mining of Ca²⁺ and H₂PO₄⁻ ions by plants.

4. Conclusion

Polymer nano-composite phosphate fertilizer was prepared by grafting partially neutralized acrylic acid onto cellulose backbone in presence of nano-HA. Nano-HA content enhanced hydrophilicity of polymer nano-composite to an optimal SEQ value of 120 (g/g) at 2.5% w/v, after which it declined. FTIR analysis indicated existence of chemical interactions between the nano-HA and the copolymer structure. Synthesis of nano-HA in presence of a surfactant led to the formation of rod-shaped nano-crystals. The main constituents of the polymer nano-composite are C, O, Ca & P. N could not be detected with EDX spectroscopic technique. The X-ray analysis indicated that, dry cellulose was in the form of cellulose I crystalline allomorph. Diffractogram of cellulose grafted copolymer displayed a more of amorphous pattern compared to that of dry water hyacinth cellulose. Besides being part of the copolymer network, nano-HA crystals were entrapped within the network structure increasing the mechanical strength and hence making it a feasible source of slow release P upon degradation and solubilization. This could subsequently enhance P use efficiency and safe handling of nano-particles, reduce production cost and environmental contamination, as well as condition the soil due to increased moisture holding capacity.

Acknowledgments

The authors acknowledge DAAD (Germany) and National Research Fund (NRF, Kenya) for financial assistance, and University of Nairobi staff Mr. Evans Kimega and Ms. Rose Mutungi for technical assistance.

References

- [1] M.S. Hashem, A.M. El-Hady, A. Hebeish, Synthesis and characterization of novel carboxymethyl cellulose hydrogels and carboxymethyl cellulose-hydrogel-ZnO-nanocomposites, *Carbohydr Polym* 95 (2013) 421–427, <https://doi.org/10.1016/j.carbpol.2013.03.013>.
- [2] M. Baki, J. Abedi-Koupai, Preparation and characterization of a superabsorbent slow-release fertilizer with sodium alginate and biochar, *J. Appl. Polym. Sci.* 135 (2017), 45966. <https://doi.org/10.1002/app.45966>.
- [3] P. Milani, D. França, A.G. Balieiro, R. Faez, Polymers and its applications in agriculture, *Polímeros* 27 (3) (2017) 256–266, <https://doi.org/10.1590/0104-1428.09316>.
- [4] M. Tally, Y. Atassi, Optimized synthesis and swelling properties of a pH-sensitive semi-IPN superabsorbent polymer based on sodium alginate-g-poly(acrylic acid-co-acrylamide) and polyvinylpyrrolidone and obtained via microwave irradiation, *J. Polym. Res.* 22 (2015) 181, <https://doi.org/10.1007/s10965-015-0822-3>.
- [5] G. Mahdavinia, A. Afzali, H. Etemadi, H. Hosseinzadeh, Magnetic/pH-sensitive nano-composite hydrogel based carboxymethyl cellulose-g-polyacrylamide/montmorillonite for colon targeted drug delivery, *Nanomater Res J* 2 (2) (2017) 111–122, <https://doi.org/10.22034/nmrj.2017.58964.1058>.
- [6] A. Martinez-Ruvalcaba, J.C. Sanchez-Diaz, A. Gonzalez-Alvarez, Polyacrylamide-gelatin polymeric networks: effect of pH and gelatin concentration on the swelling kinetics and mechanical properties, *Polym Bull* 62 (2009) 539–548, <https://doi.org/10.1007/s00289-008-0037-4>.
- [7] R.A. Hussien, A.M. Donia, A.A. Atia, O.F. El-Sedfy, A.R. Abd El-Hamid, R.T. Rashad, et al., Studying some hydro-physical properties of two soils amended with

- kaolinite-modified cross-linked polyacrylamides, *Catena* 92 (2012) 172–178, <https://doi.org/10.1016/j.catena.2011.12.010>.
- [8] M. Sadeghi, S. Safari, H. Shahsavari, H. Sadeghi, F. Soleimani, Effective parameters onto graft copolymer based on carboxymethyl with acrylic monomer, *Asian J. Chem.* 25 (9) (2013) 5029–5032.
- [9] C. Demitri, F. Scalera, M. Madaghiele, A. Sannino, A. Maffezzoli, Potential of cellulose-based superabsorbent hydrogels as water reservoir in agriculture, *Int J Polym Sci* (2013) <https://doi.org/10.1155/2013/435073>.
- [10] W.A. Laftah, S. Hashim, A.N. Ibrahim, Polymer hydrogels: a review, *Polym.-Plast. Technol. Eng.* 50 (14) (2011) 1475–1486.
- [11] E.M. Ahmed, Hydrogel: preparation, characterization and applications: a review, *J. Adv. Res.* 6 (2) (2015) 105–121, <https://doi.org/10.1016/j.jare.2013.07.006>.
- [12] A.S. Giroto, G.F. Guimarães, M. Foschini, C. Ribeiro, Role of slow-release nanocomposite fertilizers on nitrogen and phosphate availability in soil, *Sci. Report.* 7 (2017), 46032.
- [13] G.B. Marandi, G.R. Mahdavinia, S. Ghafary, Collagen-g-poly(sodium acrylate-co-acrylamide)/sodium montmorillonite superabsorbent nanocomposites: synthesis and swelling behavior, *J. Polym. Res.* 18 (2011) 1487–1499, <https://doi.org/10.1007/s10965-010-9554-6>.
- [14] A. Bortolin, F.A. Aouada, L.H.C. Mattoso, C. Ribeiro, Nanocomposite PAAm/methyl cellulose/montmorillonite hydrogel: evidence of synergistic effects for the slow release of fertilizers, *J. Agric. Food Chem.* 61 (31) (2013) 7431–7439, <https://doi.org/10.1021/jf401273n>.
- [15] S.R. Shirsath, A.P. Hage, M. Zhou, S.H. Sonawane, M. Ashokkumar, Ultrasound assisted preparation of nanoclay bentonite-FeCo nanocomposite hybrid hydrogel: a potential responsive sorbent for removal of organic pollutant from water, *Desal* 281 (2011) 429–437, <https://doi.org/10.1016/j.desal.2011.08.031>.
- [16] Y. Deng, L. Wang, X. Hu, B. Liu, Z. Wei, S. Yang, et al., Highly efficient removal of tannic acid from aqueous solution by chitosan coated attapulgite, *Chem. Eng. J.* 181–182 (2012) 300–306, <https://doi.org/10.1016/j.cej.2011.11.082>.
- [17] A. Rashidzadeh, A. Olad, D. Salari, A. Reyhanitabar, On the preparation and swelling properties of hydrogel nanocomposite based on sodium alginate-g-poly (acrylic acid-co-acrylamide)/clinoptilolite and its application as slow release fertilizer, *J. Polym. Res.* 21 (2014) 344, <https://doi.org/10.1007/s10965-013-0344-9>.
- [18] WRB (World Reference Base) for Soil Resource, International soil classification for naming soils and creating legends for maps, *World Soil Resour Rep* (2015) 106.
- [19] R. Lui, R. Lal, Synthetic apatite nanoparticles as a phosphorus fertilizer for soybean (*Glycine max*), *Sci Rep: Environ Sci* 4 (2014) 5686, <https://doi.org/10.1038/srep05686>.
- [20] D. Montalvo, M.J. McLaughlin, F. Degryse, Efficacy of hydroxyapatite nanoparticles as phosphorus fertilizers in andisols and oxisols, *Soil Sci. Soc. Am. J.* 79 (2015) 551–558, <https://doi.org/10.2136/sssaj2014.09.0373>.
- [21] K. Rop, D. Mbui, N. Njomo, G.N. Karuku, I. Michira, R.F. Ajayi, Biodegradable water hyacinth cellulose-graft-poly(ammonium acrylate-co-acrylic acid) polymer hydrogel for potential agricultural application, *Heliyon.* 5 (2019), e01416. <https://doi.org/10.1016/j.heliyon.2019.e01416>.
- [22] K. Rop, G.N. Karuku, D. Mbui, I. Michira, N. Njomo, Formulation of slow release NPK fertilizer (cellulose-graft-poly (acrylamide)/nano-hydroxyapatite/soluble fertilizer) composite and evaluating its N mineralization potential, *Annal. Agric. Sci.* 63 (2018) 163–172, <https://doi.org/10.1016/j.aoas.2018.11.001>.
- [23] D. Roy, M. Semsarilar, J. Guthriea, S. Perrier, Cellulose modification by polymer grafting: a review, *RSC Chem Soc Rev* 38 (7) (2009) 1825–2148.
- [24] D. Swantomo, B.K. Rochmadi, R. Sudiyo, Synthesis and characterization of graft copolymer rice straw cellulose-acrylamide hydrogels using gamma irradiation, *Atom Indonesia* 39 (2) (2013) 57–62.
- [25] R. Pönni, Changes in accessibility of cellulose for kraft pulps measured by deuterium exchange, *Aalto Univ Publ Ser, Doc Dissert* 68 (2014).
- [26] J. Gao, B. Huang, J. Lei, Z. Zheng, Photografting of methacrylic acid onto hydroxyapatite particles surfaces, *J. Appl. Polym. Sci.* 115 (2010) 2156–2161, <https://doi.org/10.1002/app.31307>.
- [27] H. Hosseinzadeh, M. Sadeghi, Preparation and swelling behaviour of carboxymethyl cellulose-g-poly(sodium acrylate)/kaolin super absorbent hydrogel composites, *Asian J. Chem.* 24 (2012) 85–88.
- [28] E. Iyyappan, P. Wilson, Synthesis of nanoscale hydroxyapatite particles using Triton X-100 as an organic modifier, *Ceram. Int.* 39 (2013) 771–777, <https://doi.org/10.1016/j.ceramint.2012.06.090>.
- [29] A. Costescu, I. Pasuk, F. Ungureanu, A. Dinischiotu, M. Costache, F. Huneau, et al., Physico-chemical properties of nano-sized hexagonal hydroxyapatite powder synthesized by sol-gel, *Digest J Nanomat Biostruct* 5 (4) (2010) 989–1000.
- [30] O.G. Cisneros-Pineda, W.H. Kao, M.I. Loria-Bastarrachea, Y. Veranes-Pantoja, J.V. Cauich-Rodríguez, J.M. Cervantes-Uc, Towards optimization of the silanization process of hydroxyapatite for its use in bone cement formulations, *Mat Sci Eng: C* 40 (2014) 157–163, <https://doi.org/10.1016/j.msec.2014.03.064>.
- [31] B. Gayathri, N. Muthukumarasamy, D. Velauthapillai, S.B. Santhosh, V. Asokan, Magnesium incorporated hydroxyapatite nanoparticles: preparation, characterization, Antibacterial and Larvicidal Activity, *Arab J Chem* 11 (2018) 645–654, <https://doi.org/10.1016/j.arabjch.2016.05.010>.
- [32] N. Pramanik, D. Mishra, I. Banerjee, T.K. Maiti, P. Bhargava, P. Pramanik, Chemical synthesis, characterization, and biocompatibility study of hydroxyapatite/chitosan phosphate nanocomposite for bone tissue engineering applications, *Int J Biomater* (2009) <https://doi.org/10.1155/2009/512417> Article ID 512417.
- [33] A. Ragu, P. Sakthivel, Synthesis and characterization of nanohydroxyapatite with polymethyl methacrylate nanocomposites for bone tissue regeneration, *Int J Sci Res* 3 (11) (2014) 2282–2285.
- [34] Liao Y. Practical electron microscopy and database. <http://www.globalsino.com/EM/>; 2006 [accessed 20th August 2019].
- [35] M. Ago, T. Endo, T. Hirotsu, Crystalline transformation of native cellulose I to cellulose II polymorph by a ball milling method with specific water, *Cellulose* 11 (2004) 163–167, <https://doi.org/10.1023/B:CELL.0000025423.32330.0a>.
- [36] G. Chen, P. Varanasi, C. Li, H. Liu, Y.B. Melnichenko, B.A. Simmons, et al., Transition of cellulose crystalline structure and surface morphology of biomass as a function of ionic liquid pretreatment and its relation to enzymatic hydrolysis, *Biomacromol* 12 (4) (2011) 933–941, <https://doi.org/10.1021/bm101240z>.
- [37] H. Bai, X. Wang, Y. Zhou, L. Zhang, Preparation and characterization of poly(vinylidene fluoride) composite membranes blended with nano-crystalline cellulose, *Prog Nat Sci: Mat Int* 22 (3) (2012) 250–257, <https://doi.org/10.1016/j.pnsc.2012.04.011>.
- [38] H.A. Ambjörnsson, Mercerization and enzymatic pretreatment of cellulose in dissolving pulps, *Dissert Karlstad Univ* 22 (2013), ISSN 1403-8099 <https://www.diva-portal.org/smash/get/diva2:616374/FULLTEXT01.pdf>.
- [39] P.K. Gupta, V. Uniyal, S. Naithani, Polymorphic transformation of cellulose I to cellulose II by alkali pretreatment and urea as an additive, *Carbohydr Polym* 94 (2013) 843–849, <https://doi.org/10.1016/j.carbpol.2013.02.012>.
- [40] S. Nam, A.D. French, B.D. Condon, M. Concha, Segal crystallinity index revisited by the simulation of X-ray diffraction patterns of cotton cellulose I β and cellulose II, *Carbohydr Polym* 135 (2016) 1–9.
- [41] A. Mechay, H.L. Feki, F. Schoenstein, N. Jouini, Nanocrystalline hydroxyapatite ceramics prepared by hydrolysis in polyol medium, *Chem Phys Lett* 541 (2012) 75–80, <https://doi.org/10.1016/j.cplett.2012.05.047>.
- [42] R.K. Brundavanam, G.E.J. Poinern, D. Fawcett, Modelling the crystal structure of a 30 nm sized particle based hydroxyapatite powder synthesised under the influence of ultrasound irradiation from X-ray powder diffraction data, *Am J Mat Sci* 3 (4) (2013) 84–90, <https://doi.org/10.5923/j.materials.20130304.04>.
- [43] K. Rop, G.N. Karuku, D. Mbui, N. Njomo, I. Michira, Evaluating the effects of formulated nano-NPK slow release fertilizer composite on the performance and yield of maize, kale and capsicum, *Annal Agric Sci* 64 (2019) 9–19, <https://doi.org/10.1016/j.aoas.2019.05.010>.
- [44] M.S. Khan, A. Zaidi, E. Ahmad, Mechanism of phosphate solubilization and physiological functions of phosphate-solubilizing microorganisms, in: M.S. Khan, A. Zaidi, J. Musarrat (Eds.), *Phosphate Solubilizing Microorganisms*, Springer, Cham, 2014 https://doi.org/10.1007/978-3-319-08216-5_2.
- [45] E.T. Alori, B.R. Glick, O.O. Babalola, Microbial phosphorus solubilization and its potential for use in sustainable agriculture, *Front. Microbiol.* 8 (2017) 971, <https://doi.org/10.3389/fmicb.2017.00971>.